Interfacial and Distal-Heme Pocket Mutations Exhibit Additive Effects on the Structure and Function of Hemoglobin†

David H. Maillett,‡ Virgil Simplaceanu,‡ Tong-Jian Shen,‡ Nancy T. Ho,‡ John S. Olson,§ and Chien Ho*,‡

Department of Biological Sciences, Carnegie Mellon University, Pittsburgh, Pennsylvania 15213, and Department of Biochemistry and Cell Biology, Rice University, Houston, Texas 77025

Received May 5, 2008; Revised Manuscript Received August 4, 2008

ABSTRACT: Protein engineering strategies seek to develop a hemoglobin-based oxygen carrier with optimized functional properties, including (i) an appropriate O_2 affinity, (ii) high cooperativity, (iii) limited NO reactivity, and (iv) a diminished rate of auto-oxidation. The mutations αL29F, αL29W, αV96W and βN108K individually impart some of these traits and in combinations produce hemoglobin molecules with interesting ligand-binding and allosteric properties. Studies of the ligand-binding properties and solution structures of single and multiple mutants have been performed. The aromatic side chains placed in the distal-heme pocket environment affect the intrinsic ligand-binding properties of the mutated subunit itself, beyond what can be explained by allostery, and these changes are accompanied by local structural perturbations. In contrast, hemoglobins with mutations in the $\alpha_1\beta_1$ and $\alpha_1\beta_2$ interfaces display functional properties of both "R"- and "T"-state tetramers because the equilibrium between quaternary states is altered. These mutations are accompanied by global structural perturbations, suggesting an indirect, allostery-driven cause for their effects. Combinations of the distal-heme pocket and interfacial mutations exhibit additive effects in both structural and functional properties, contribute to our understanding of allostery, and advance protein-engineering methods for manipulating the O_2 binding properties of the hemoglobin molecule.

Human hemoglobin (Hb[1]) serves as a classical model of allostery in proteins, and its study has contributed greatly to understanding the relationship between structure and function in biological molecules. The two-state model of allostery in proteins described by Monod, Wyman and Changeux was based, in part, on structural and functional studies in Hb (*1*). According to this two-state model, cooperative O_2 binding results from a conversion of Hb between high affinity "R"- and low affinity "T"-states, and allosteric control operates by changing the equilibrium between these two states, measured as the equilibrium constant, *L*. Comparison of X-ray crystal structures of Hb allowed Perutz to assign R- and T-states to quaternary structures of the Hb tetramer and establish a stereochemical description of allostery that has been widely used in explaining and understanding cooperative O_2 binding by Hb (*2*).

A large amount of work suggests that a simple two-state mechanism does not fully account for cooperativity and allostery in O_2 binding. Structural studies have detected conformations of Hb distinct from those originally noted, including R2 (*3*), RR2 and R3 (*4*) conformations. NMR studies suggest that the solution structure of HbCO A is a dynamic intermediate between R and R2 conformations (*5*), with the R structure representing an intermediate form between T and R2 structures (*6*), consistent with the pathway proposed by Srinivasan and Rose (*7*). Alternate structures may fit with a two-state model, but only if the structural ensemble sorts into only two functional states. The low-affinity T-state form of Hb appears to comprise at least two different forms with differing affinities (*8, 9*). Trapping these states in a sol−gel has allowed detection of functional behaviors intermediate between classic R- and T-state traits (*10*). Numerous high-quality X-ray crystal structures have been reported for deoxy-Hb, but none appear to match the solution structure, which could possibly represent rapidly interconverting species (*11*). To account for inadequacies of the original two-state model, several new models of allostery in hemoglobin have been proposed including the global allostery (*12, 13*), molecular code (*14*−*16*) and tertiary-two state (*17*) models.

Understanding of allostery in Hb can be advanced by the study of mutant recombinant Hbs (rHbs) possessing interesting new structural or functional properties. Such rHbs are being produced in a rational protein engineering approach to develop a hemoglobin-based oxygen carrier (HBOC). Promising rHbs should possess (i) appropriate O_2 affinity, in order to facilitate O_2 delivery in the absence of the

† This work is supported by research grants from the National Institutes of Health (R01HL-024525 and R01GM-084614 in support of V.S., T.-J.S., N.T.H. and C.H., and HL-047020, GM 35649, and Welch Foundation Grant C-0612 in support of J.S.O.), and D.H.M. was supported by a postdoctoral fellowship sponsored by the American Heart Association (0625507U).

* Address all correspondence to Dr. Chien Ho, Department of Biological Sciences, Carnegie Mellon University, 4400 Fifth Avenue, Pittsburgh, PA 15213. Tel: 412-268-3395. Fax: 412-268-7129. E-mail: chienho@andrew.cmu.edu.

‡ Carnegie Mellon University.

§ Rice University.

[1] Abbreviations: Hb, hemoglobin; Mb, myoglobin; rHb, recombinant hemoglobin; rMb, recombinant myoglobin; D_2O, deuterium oxide; ns, nanosecond; OEC, oxygen equilibrium curve; 2,3-BPG, 2,3 bisphosphoglycerate; HBOC, hemoglobin-based oxygen carrier; IHP, inositol hexaphosphate; DSS, 2,2-dimethyl-2-silapentane-5-sulfonic acid; ΔMAP, change in mean arterial pressure.

10.1021/bi800816v CCC: $40.75
Published on Web 09/13/2008

intracellular allosteric effector, 2,3-bisphosphoglycerate (2,3-BPG); (ii) resistance to auto-oxidation, in order to increase the functional half-life of the product and inhibit the production of radical oxygen species; and (iii) limited reactivity with nitric oxide (NO) to diminish the "hypertensive side effect" (*18*). Hbs containing αL29F, αL29W, αV96W, and βN108K substitutions possess many of these desirable qualities.

Hb Presbyterian, containing the βN108K substitution, was first found in three generations of the same family (*19*). Incorporation of this mutation into rHb conferred (i) a pronounced chloride effect; (ii) an enhanced Bohr effect; (iii) lowered O_2 affinity; and (iv) the capacity to switch to the low-affinity T-state conformation without changing ligation state (*20*). Acharya and co-workers found that the unusual T-state like character of the liganded form of transgenic (Tg) Hb (βN108K) is (i) detectable as an increase in geminate yield of carbon monoxide; (ii) enhanced by the allosteric effector phosphate; and (iii) manifested at both "hinge" and "switch" regions of the $\alpha_1\beta_2$ interface, while the structure of the deoxygenated form is unperturbed compared to Hb A (*21*). Properties of Hb Presbyterian, including decreased O_2 affinity and increased Bohr effect, facilitate O_2 delivery and led the research group at Somatogen to use the βN108K mutation in their first-generation rHb-based blood substitute product, rHb1.1 (*22, 23*). This group believed, as do we, that low affinity (P_{50} between 20 and 30 Torr) enhances O_2 delivery, in both *in vitro* and *in vivo* conditions (*24, 25*). In contrast to this view is the belief that higher O_2 affinity is required in a HBOC in order to prevent premature O_2 delivery and overcompensation in autoregulation of capillary flow (*26*).

The αV96W substitution within the $\alpha_1\beta_2$ interface that was created and characterized by our laboratory was found to increase P_{50} (*27*). Unlike many mutations within the $\alpha_1\beta_2$ interface that disrupt H-bond or salt-bridge interactions and result in high O_2 affinity and low cooperativity, the αV96W substitution lowers O_2 affinity while maintaining high cooperativity. We have found that the CO bound form could adopt the T-type quaternary structure without changing ligation state upon addition of the allosteric effector inositol hexaphosphate (IHP) and/or a decrease in temperature (*27*). X-ray crystal structures have shown that this Hb creates a water-mediated H-bond network between α96W and β101E that appears to stabilize the T-state conformation, and that the R-state structure contains a β101E−β104R interaction, which is normally seen only in T-state structures (*28*).

The lowered affinity and high cooperativity of βN108K and αV96W substitutions have prompted our laboratory to explore the effect of the double mutation on the structure and function of Hb (*20*). We have found that rHb (αV96W/βN108K) has a greater tendency to switch to the T-state conformation without changing ligation state than either single mutant, and that the double mutant has a lower O_2 affinity than either single mutant. This combination of mutations appears to promote low O_2 affinity by stabilizing the T-state of Hb while destabilizing or altering the high-affinity R-state, creating a promising prototype for a blood substitute molecule with a high P_{50} value. To advance this approach, we added the B10 mutation, αL29F, to the double mutant (*29*). The L29F substitution in both myoglobin (Mb) and Hb was found previously to decrease the rates of both auto-oxidation and NO dioxygenation (*30*−*32*). However, this mutation markedly increases O_2 affinity in both Mb and Hb to levels that would preclude O_2 delivery in a normal capillary which has P_{O_2} of ∼30 to 50 Torr (*31, 33*−*35*). Thus, we have combined the αL29F mutation with the allosteric mutants to produce a rHb (αL29F/αV96W/βN108K) triple mutant with lower affinity than Hb A and lower auto-oxidation rates than rHb (αV96W/βN108K) (*29*).

Here, we present results of flash photolysis, equilibrium binding, ^{1}H NMR, and rapid-mixing studies on Hbs containing αL29F, αL29W, αV96W, βN108K, αV96W/βN108K, αL29F/αV96W/βN108K, and αL29W/αV96W/βN108K mutations. The distal-heme pocket mutations at the B10 helical position alter the intrinsic ligand binding properties of the α-subunits, whereas the interface mutants affect the allosteric equilibrium, and both types of effects are additive in the multiple mutants.

EXPERIMENTAL PROCEDURES

Hemoglobin Solutions. Recombinant hemoglobins were designed, expressed and purified according to previously described procedures (*36, 37*). The plasmids coexpress methionine aminopeptidase (Met-AP), which removes the N-terminal methionine necessary for bacterial expression and results in production of authentic Hb. An oxidation−reduction step for the rHb molecule is included in the purification procedure in order to convert incorrectly oriented heme groups to the correct orientation (for details, see refs *36, 37*).

Experimental Conditions. All experiments were performed in 0.1 M sodium phosphate buffer at pH 7.0 and 20 °C, with the exception of the geminate rebinding studies which were performed at 22 °C. Hb concentrations are reported on per heme or subunit basis.

Kinetic Measurements. Association and dissociation rate constants were determined as described previously for Hbs (*38*−*40*). Flash-photolysis experiments monitored ligand rebinding as a change in the absorbance at 436 nm following photodissociation of ∼10% of the bound ligands. Buffers equilibrated with 1 atm of O_2 (1.25 mM O_2) or 1 atm of CO (1.0 mM CO) ensured pseudo-first order conditions for the rebinding reaction to 0.1 mM Hb (heme basis). Partial photolysis was employed to produce a comparatively large population of triliganded molecules so that absorbance changes would reflect the last step of the ligand binding (i.e., $Hb_4X_3 + X \rightarrow Hb_4X_4$). Time courses were fit to a two-exponential expression, and the resulting observed rates were divided by the ligand concentration to yield association rate constants. Dependence of the observed rates on ligand concentration was confirmed by experiments performed in buffers containing 0.25 mM O_2 or 0.10 mM CO.

Rate constants for CO dissociation from the rHbs were measured by rapid mixing techniques. rHbs in solutions containing 0.1 mM CO were mixed with buffer containing 2.0 mM (equilibrated with 1 atm) nitric oxide (NO). Free NO was present in excess and has an association rate constant approximately 10-fold greater than k'_{CO} for Hb, allowing the CO-rebinding reaction to be ignored. The CO dissociation rate constants were determined for α- and β-subunits directly from the time courses by fitting with a two-exponential expression.

Rate constants for O_2 dissociation were also measured by rapid mixing techniques. In this case, 0.1 mM (heme basis)

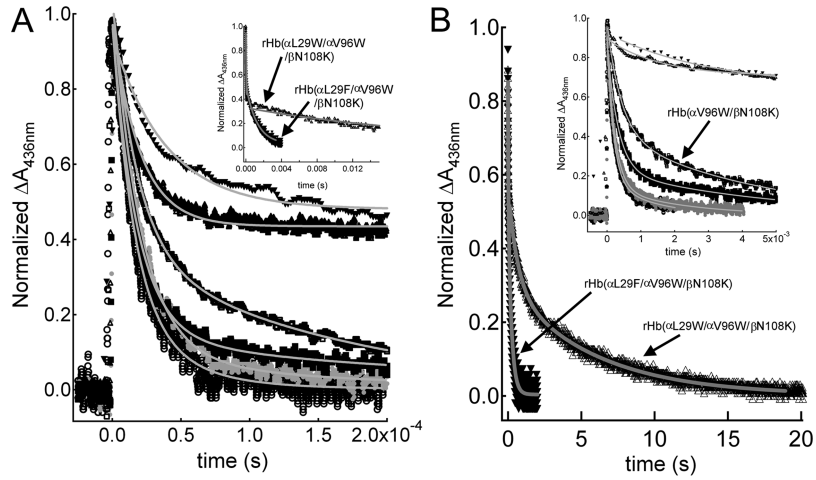

FIGURE 1: Representative time courses of ligand rebinding following partial (10%) photolysis. Lines indicate fits to one- or two-exponential functions. (A) Rebinding of 100% O_2 to native Hb A (black ●), rHb (αV96W) (gray ●), rHb (βN108K) (■), rHb (αV96W/βN108K) (□), rHb (αL29F/αV96W/βN108K) (▼), and rHb (αL29W/αV96W/βN108K) (△). Inset, rebinding on longer time scale shows the slower phase of the triple mutant rHbs. (B) Rebinding of 100% CO to the same Hbs reveals similar behaviors. Experiments were performed in 0.1 M sodium phosphate buffer at pH 7.0 and 20 °C.

Hb in buffer equilibrated with air was mixed with buffer solutions equilibrated with 1 atm of N_2, 1 atm of CO, and air using a SFM-400 stopped flow (Biologic, France). Proportions of mixing were manipulated to record a number of time courses over a range of [CO]/[O_2] values. The time courses were fit to two-exponential expressions to measure fast and slow phases. Because the O_2 rebinding reaction cannot be ignored, the rate constant, k_{RO_2}, was obtained by fitting the dependence of the observed pseudo first order replacement rate constants, r_{obs}, on [CO]/[O_2] to the following expression:

$$r_{obs} = \frac{k_{RO_2}\dfrac{[CO]}{[O_2]}}{\dfrac{[CO]}{[O_2]} + \dfrac{k'_{RO_2}}{k'_{RCO}}} \quad (1)$$

The relatively low final Hb concentration of 5 to 10 μM results in some dimer formation and an overestimation of R-state character for the low affinity mutants since the ability to switch to the T-state relies on an intact $\alpha_1\beta_2$ interface.

Equilibrium Oxygen Binding Curves. Oxygen-dissociation curves were measured using a Hemox Analyzer (TCS Medical Products, Huntington Valley, PA), as described previously (*36, 37*) with modifications. Hb concentration was 60 μM, and 0.3 μM catalase and superoxide dismutase were included to limit oxidation. Oxygen affinity, measured as P_{50}, and cooperativity, measured as the Hill coefficient (n_{50}), were determined from the resulting oxygen equilibrium curves (OECs) with an accuracy estimated at ±10% based on reproducibility of measurements with Hb A.

NMR Spectroscopy. ^{1}H NMR spectra were measured for Hbs equilibrated under 1 atm of CO gas using a 300-MHz Bruker Avance DRX-300 NMR spectrometer. Hb concentration was 4 mM (heme basis), dissolved in 0.1 M sodium phosphate pH 7.0 with 5% D_2O added. The water signal was suppressed by using a jump-and-return pulse sequence (*41*). Proton chemical shifts are referenced to the methyl proton resonance of 2,2-dimethyl-2-silapentane-5-sulfonate (DSS) indirectly by using the water signal, which occurs 4.85 ppm downfield from DSS at 20 °C, as the internal reference.

RESULTS

Measurement of Association Rates. Representative time courses for CO and O_2 rebinding following partial flash-photolysis are shown in Figure 1. In these experiments, ~10% of the bound ligand was photodissociated. As a result, the last step of ligand binding (i.e., $Hb_4X_3 + X \rightarrow Hb_4X_4$, where X is the ligand O_2 or CO) contributes virtually all of the recorded absorbance change. This measurement is model-independent. Considered within the context of the two-state MWC model, the last step of ligand binding normally represents association with the high-affinity R-quaternary state of the Hb tetramer (*1*). Fitting using two exponentials allows calculation of bimolecular ligand association rate constants $k'_{R\alpha}$ and $k'_{R\beta}$ for α- and β-chains, respectively (*25*). However, the set of mutant rHbs being examined contains substitutions which may promote low affinity T-state character in Hb, even in the fully saturated state, and thus, mixtures of k'_R and k'_T values can occur. This possibility is considered in assigning apparent rate constants for the faster and slower phases (k_f and k_s, respectively) of ligand rebinding.

Placement of Phe or Trp at position B10 of the α-subunit produced dramatic decreases in the rate of the slow phase of O_2 binding in all four mutants containing these substitutions. The scale of these reductions is greater than that seen in rMb (L29W), which produces a 70-fold decrease in k'_{O_2} compared to wild-type, and matches the large decreases in k'_{O_2} seen previously in rHb (αV1M/βV1M/αL29F) and rHb (αV1M/βV1M/αL29W) (*42, 43*). The amplitude of the markedly slower phase accounts for roughly 50% of the total observed reaction in each of the mutants containing the single distal mutation. The relatively unperturbed faster phase, stoichiometric amplitude distribution, and agreement with previous results for distal-heme pocket mutations of Hb and Mb lead to straightforward assignments of the slow and fast phases to α- and β-subunits of the Hb, respectively. Rate constants for ligand association were calculated by fitting time courses to two-exponential functions and are reported in Table 1, together with values previously reported for Hb A (*44*−*46*). Values of $k'_{R\alpha O_2}$ measured in all four samples

Table 1: Ligand Binding Parameters[a]

	O_2 binding						CO binding			
	$k'_{O_2,slow}$, μM^{-1} s^{-1}	$k'_{O_2,fast}$, μM^{-1} s^{-1}	A_{slow}	A_{fast}	$k_{O_2,slow}$, s^{-1}	$k_{O_2,fast}$, s^{-1}	$k'_{CO,slow}$, μM^{-1} s^{-1}	$k'_{CO,fast}$, μM^{-1} s^{-1}	A_{slow}	A_{fast}
Hb A '"R-state" (*44*)	36	76			16	32	6.0	7.4		
Hb A "R-state" (*45*)	28	100			12	22	2.9	7.1		
Hb A	27	73	0.51	0.49	11	32	2.4	7.1	0.48	0.52
rHb (αL29F)	**0.68**	55	0.47	0.53	**0.16**	33	***0.020***	5.5	0.71	0.29
rHb (αL29W)	***0.083***	65	0.57	0.43	**0.98**	25	***0.0037***	5.4	0.64	0.36
rHb (αV96W)	10	55	**0.09**	0.91	14	49	1.2	5.7	0.35	0.65
rHb (*β*N108K)	**4.3**	54	0.24	0.76	15	100	**0.34**	3.2	0.23	0.77
rHb (αV96W/*β*N108K)	**4.2**	43	0.36	0.64	20	120	**0.43**	2.6	0.39	0.61
rHb (αL29F/αV96W/*β*N108K)	**0.74**	26	0.49	0.51	**0.30**	48	***0.0062***	**0.084**	0.55	0.45
rHb (αL29W/αV96W/*β*N108K)	***0.035***	40	0.43	0.57	**2.2**	39	***0.00024***	***0.063***	0.46	0.54
Hb A "T-state" (*45*)	5.6	6.7			430	670	0.16	0.07		
Hb A "T-state" (*46*)	4.8	7.5			2000	2000	0.15	0.15		

[a] Changes of 5- and 100-fold from native Hb A are indicated in bold and bold italics. Conditions: 0.1 M sodium phosphate buffer pH 7.0, 20 °C.

containing aromatic side chains substituted into the distal binding pocket are ~10- to 100-fold smaller than the reported values of $k'_{T\alpha O_2}$, indicating that the effect cannot be explained by allostery alone. The αL29F and αL29W mutations directly alter the intrinsic ligand-binding properties of the α-subunit, and that effect is clearly conserved in the multiple mutants.

Similar experiments were performed using CO as the ligand, as illustrated in Figure 1B. Again, the time courses are markedly biphasic and exhibit a slow-phase rate constant, which is 10- to 300-fold lower than the reported T-state values, making the assignment of the mutant B10 α-subunit phase straightforward. This shows that the distal-heme pocket substitutions interfere with ligand association in a ligand-independent fashion. Calculated rate constants are presented in Table 1. Interestingly, the rate constants for the faster phase of CO rebinding in the rHb (αL29F/αV96W/*β*N108K) and rHb (αL29W/αV96W/*β*N108K) triple mutants match those reported for $k'_{T\beta CO}$ rather than $k'_{R\beta CO}$ suggesting that even with only 10% photolysis, the Hb tetramers are still in the T or low affinity quaternary state. This pattern differs from that seen with the same rHbs using O_2 as ligand, or that seen in the single rHb (αL29F) and rHb (αL29W) mutants that do appear to switch to the R-state when three ligands have been bound. Thus, the T-quaternary conformation may occur for the $Hb_4(CO)_3$ species during the partial photolysis experiments.

To test this idea, the time courses following full photolysis have been analyzed. In the case of Hb A, full photolysis allows a significant fraction of the unliganded tetramers to switch quaternary conformations during the dye laser pulse, leading to biphasic rebinding time courses with slower apparent rate constants due to the presence of a large fraction of tetramers in the T-state quaternary form. In the case of the triple mutants, the fast and slow rate constants measured for CO binding after full photolysis are nearly identical to the rate constants determined after 10% photolysis. The full photolysis values are 0.003 and 0.11 μM^{-1} s^{-1} for rHb (αL29F/αV96W/*β*N108K) and 0.0002 and 0.03 μM^{-1} s^{-1} for rHb (αL29W/αV96W/*β*N108K), and can be compared to the partial photolysis values reported in Table 1. The lack of dependence of the measured rate constants on the degree of photolysis and the excellent agreement between the faster phase and reported values of $k'_{T\beta CO}$ demonstrate that these triple mutant Hbs exhibit functional properties of the T quaternary state, even with three ligands bound [$Hb_4(CO)_3$]. Such T-state behavior was not seen in the single αL29 mutants, showing that the combined αV96W and *β*N108K substitutions cause retention of the T-state in triliganded intermediates. The appearance of the T-state functional properties after partial photolysis of the two triple mutants arises from a quaternary switch to the low affinity form in the newly produced $Hb_4(CO)_3$ intermediate, which has time to occur due to ultraslow CO rebinding to the B10 mutants.

The *β*N108K single mutant exhibits a fast O_2 rebinding phase after partial photolysis, with a rate constant of 54 μM^{-1} s^{-1}, and a slower phase with a rate constant of 4.3 μM^{-1} s^{-1}. Assignments based on these time courses alone are not straightforward. The apparent rate constant of the faster phase is similar to the average of the two R-state subunit association rate constants. The apparent rate constant for the slower phase, 4.3 μM^{-1} s^{-1}, is similar to that for O_2 binding to the T-state subunits and suggests that this mutation by itself can slow down the rate of the last step in ligand binding by creating a population of $Hb_4(O_2)_3$ tetramers in the T-quaternary conformation. The amplitudes of the fast and slow phases of rebinding support this interpretation. Following partial photolysis of native HbCO A, the fast and slow phases of bimolecular rebinding contribute roughly equally to the total absorbance change. These phases arise from reactions of the α- and *β*-subunits, which are similar in both (i) spectral changes between liganded and unliganded states and (ii) geminate recombination yield. The slower phase of the *β*N108K mutant rebinding time course comprises only ~25% of the total signal, indicating that the phases are not due to roughly equal contributions of α- and *β*-subunits as was seen in Hb A, rHb (αL29F), and rHb (αL29W). Instead, this slow phase probably reflects the appearance of T-state character in the $Hb_4(O_2)_3$ species.

The T-state of Hb A has very low (≤1%) CO rebinding geminate yield and a high overall quantum yield (~1.0) for complete photodissociation (*47*). Thus, the presence of any T-state conformations will be amplified in partial photolysis experiments since the quantum yield for the R-state hemoglobin is roughly 0.7. Thus, in our view, the partial photolysis results for rHb (*β*N108K) indicate the presence of a major population of tetramers rebinding at the average value of k'_{RO_2} (i.e., at R-state tetramer rates), mixed with a smaller

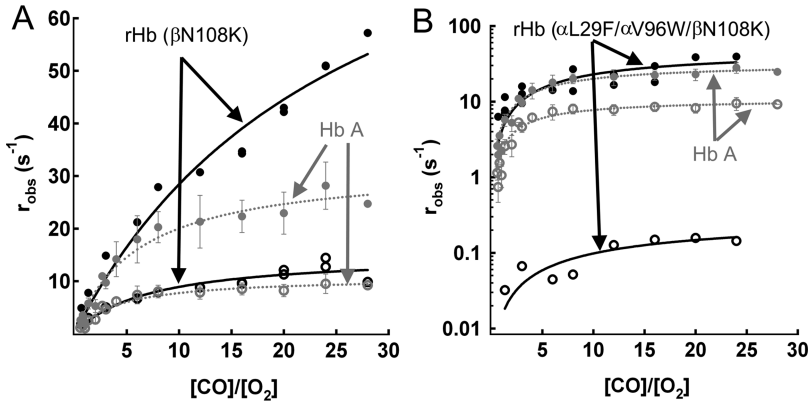

FIGURE 2: Fits of eq 1 to observed rates (r_{obs}) of O_2 replacement for two representative rHbs. Fast (●) and slow (○) phases of O_2 dissociation from Hb A are compared to (A) rHb (βN108K), which exhibits a faster fast phase, and (B) rHb (αL29F/αV96W/βN108K), which exhibits a markedly slower slow phase. A log scale for the abscissa was employed in panel B. Experiments were performed in 0.1 M sodium phosphate buffer at pH 7.0 and 20 °C.

fraction of molecules reacting at slow T-state like rate constants. This interpretation is also supported by full photolysis experiments in which 100% of the O_2 is photodissociated and the two phases of rebinding occur at average R- and T-state rates. For rHb (βN108K), k_{slow} and k_{fast} following full photolysis were measured as 6.0 and 45 μM^{-1} s^{-1}, respectively. These values agree well with rate constants of 4.3 and 54 μM^{-1} s^{-1} measured in the partial photolysis experiments. Both full and partial photolysis results agree well with previously reported average rate constants of approximately 6 and 60 μM^{-1} s^{-1} for the T- and R-state O_2 association to Hb A, respectively, as shown in Table 1.

Rebinding of CO to rHb (βN108K) produces fast and slow phases with apparent rate constants of 3.2 μM^{-1} s^{-1} and 0.34 μM^{-1} s^{-1}. As with O_2 association, the rate constants for these two phases are similar to reported values of the last (R-state like) and first (T-state like) steps of CO binding, respectively. The fractions of fast and slow phases of the total absorbance change were 0.77 and 0.23, respectively, in rHb (βN108K), and not equal as is observed in Hb A. Thus, the effects of mutation on rebinding are consistent for O_2 and CO. Apparent rate constants for fast and slow phases presented in Table 1 reflect the R- and T-state behavior and not different subunits.

Similar behavior was observed for the αV96W mutant. O_2 rebinding time courses exhibit a large amplitude phase, with an apparent rate constant that matches the average of R-state α- and β-subunit rate constants, and a smaller amplitude slow phase reflecting T-state rebinding. Least-squares fitting of partial photolysis O_2 rebinding traces produced an average slow phase rate constant of 10 μM^{-1} s^{-1}. The full photolysis time courses provided apparent rate constants of 10 and 60 μM^{-1} s^{-1}. As was also seen with rHb (βN108K), the major difference between full and partial photolysis time courses is an increase in the relative amplitude of the slow phase with increasing photolysis. CO rebinding to rHb (αV96W) shows time courses similar to those for the O_2 rebinding, including a slow T-state-like phase with a small amplitude. After full photolysis, the two rate constants for CO binding to rHb (αV96W) were 0.15 and 5.9 μM^{-1} s^{-1} in excellent agreement with those for the T- and R-state of Hb A.

O_2 rebinding to rHb (αV96W/βN108K) also proceeds in two phases with rate constants of 43 and 4.1 μM^{-1} s^{-1}. These values are nearly identical to those measured for rHb (βN108K), and the same R vs T trend is observed for k'_{CO}. The effects of the αV96W and βN108K mutations are additive on the amplitude of the slower phase. The slow phases for bimolecular O_2 rebinding to rHb (αV96W), rHb (βN108K), and rHb (αV96W/βN108K) accounted for 9, 24, and 36% of the observed absorbance change, respectively, after partial photolysis, with the double mutant, as expected, showing the greatest extent of T-state behavior.

Measurement of Dissociation Rates. Dissociation rate constants were determined by observing displacement of ligands in rapid-mixing mixing experiments. For the O_2 dissociation reaction, replacement of O_2 from HbO_2 by CO was monitored after mixing at a variety of ratios of free ligands. The time courses were fitted to a two-exponential function, and the dependence of observed rates (r_{obs}) on ligand ratio was used to determine k_{O_2} (Figure 2). Assignment of the resultant rate constants was straightforward for each sample since at least one phase matched rate constants previously reported for the α- and β-subunits, and in these experiments the starting liganded state is $Hb_4(O_2)_4$, which even in the case of the $\alpha_1\beta_2$ interface mutants normally exhibits R-state like properties.

Placement of Phe at the B10 position within the distal-heme pocket produces dramatic 70- and 40-fold decreases in k_{O_2} for α-subunits within tetrameric rHb (αL29F) and rHb (αL29F/αV96W/βN108K), respectively, compared to α-subunits within Hb A. This finding parallels the effect seen in Mb, where the L29F mutation caused a dramatic ~10-fold reduction in k_{O_2} compared to the wild-type value (*30*). The effect in Mb was explained as due to electrostatic stabilization of bound O_2 by the positive edge of the phenyl-ring multipole. This phenomenon appears to be conserved in α-subunits, where the L29F substitution reduces k_{O_2} more dramatically than in Mb. Placement of Trp at position 29 of α-subunits within tetrameric rHb (αL29W) and rHb (αL29W/αV96W/βN108K) lowered k_{O_2} in α-subunits to a much lesser extent, 10- and 5-fold, respectively, than the αL29F mutation. Again, similar effects of the Leu(B10)Trp mutation are seen for single mutants of Mb and Hb A (*25, 42, 48*). The faster phase for O_2 dissociation from each of the four samples containing aromatic substitutions within the α-subunit distal-heme pocket matched the rate constant measured for the native β-subunit, reflecting R-state type function.

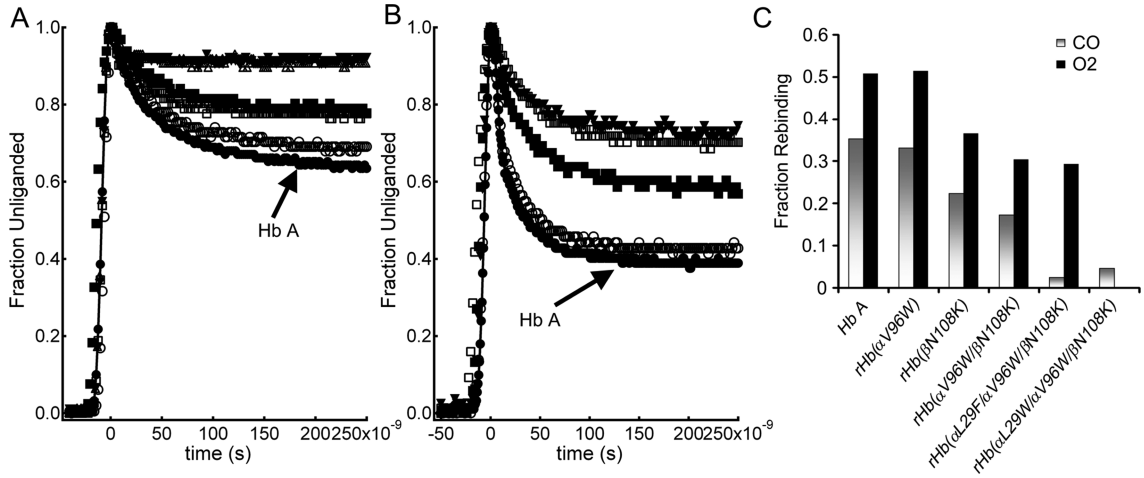

FIGURE 3: Representative time courses of geminate recombination following flash photolysis. (A) Rebinding of 100% CO to native Hb A (●), rHb (αV96W) (○), rHb (βN108K) (■), rHb (αV96W/βN108K) (□), rHb (αL29F/αV96W/βN108K) (▼), and rHb (αL29W/αV96W/βN108K) (△). (B) Rebinding of 100% O_2 to the same Hbs. (C) Fraction of O_2 and CO geminate recombination observed in each mutant is shown. The O_2 experiment using rHb (αL29W/αV96W/βN108K) is excluded due to oxidation and hemichrome formation within the sample. Experiments were performed in 0.1 M sodium phosphate buffer at pH 7.0 and room temperature.

The slower phase of the ligand dissociation reaction for rHb (αV96W), rHb (βN108K), and rHb (αV96W/βN108K) (14, 15, and 16 s^{-1}, respectively), matches the values of 12 and 16 s^{-1} previously reported for the native α-subunit of Hb A, leading to straightforward assignments. The amplitudes of the slow and fast phases are roughly equal for Hb A and rHb (αV96W). However, the replacement reactions in rHb (βN108K) and rHb (αV96W/βN108K) have a larger, ~65%, fast phase and ~3-fold larger rate constants, indicating that the βN108K interface mutation acts to facilitate O_2 dissociation, either by increasing the intrinsic rate of O_2 dissociation from the β-subunits and/or by conferring the T-state behavior to the fully oxygenated tetramer. The distal-heme pocket mutations suppress this effect, suggesting that the elevation in k_{O_2} is not due to an intrinsic change to the β-subunit itself, but instead is due to increased T-state character imparted by βN108K mutation.

Similar rapid-mixing experiments were employed to measure the replacement of bound CO through competition with NO. In this case, the high relative concentration of NO, the high association rate constants of NO, and low dissociation rate constants for NO allow direct observation of k_{CO} (*49*). Time courses were fitted to a two-exponential function using equal amplitudes, and the apparent rate constants uniformly match those of Hb A. This indicates that the effect of the βN108K substitution on ligand dissociation, unlike its effect on association, is ligand-dependent.

Measurement of Geminate Rebinding. After rapid photolysis of bound ligand from the heme group, a portion of the dissociated ligands rebind internally to the iron atom to which it was originally bound (i.e., a geminate pair). The rate and amplitude of this ultrafast, nanosecond geminate rebinding process is dependent on the ability of the surrounding protein structure to capture the ligand in apolar cavities or to eject it into the solvent phase by steric hindrance (*50*). Normalized CO and O_2 geminate rebinding traces are presented in Figure 3 and show clear differences in the fraction geminate rebinding (F_{gem}). The overall trend for F_{gem} is rHb (αL29F/αV96W/βN108K) ≈ rHb (αL29W/αV96W/βN108K) < rHb (αV96W/βN108K) < rHb (βN108K) < rHb (αV96W) ≈ Hb A and is summarized in panel C of Figure 3.

Table 2: Equilibrium Binding Parameters of Hb A and rHbs[a]

hemoglobin	P_{50} (Torr)	n_{50}
Hb A	8.0	3.0
rHb (αL29F)	4.0	2.6
rHb (αL29W)	28	2.1
rHb (αV96W)	13	2.5
rHb (βN108K)	28	2.4
rHb (αV96W/βN108K)	39	1.8
rHb (αL29F/αV96W/βN108K)	23	1.3
rHb (αL29W/αV96W/βN108K)	120	0.9

[a] Conditions: 0.1 M sodium phosphate buffer pH 7.0, 20 °C.

The alteration in F_{gem} for rHb (αV96W), rHb (βN108K) and rHb (αV96W/βN108K) reflects a decrease in iron reactivity and iron−ligand bond formation by proximal restraints of in plane movement of the iron atom as result of these substitutions at the subunit interfaces. The effects of the two interface mutations are roughly additive in the double mutant. Dramatic decreases in geminate rebinding have been observed in rHb (αV1M/βV1M/αL29F) and rHb (αV1M/βV1M/αL29W) (*42*), and it was expected that these substitutions in the distal-heme binding pocket would cause the same effect in the triple mutants. However, the observed reduction in CO geminate recombination to <10% is more severe than was found in the single αL29F and αL29W mutants and reflects the decrease in iron reactivity due to the greater T-state character caused by the interface mutants. The allosteric transition in Hb has a pronounced effect on the CO geminate reaction reducing the population of rebinding from ~40% in the R-quaternary structure to <1% for the T-state (*47*).

Measurement of Oxygen Equilibrium Curves. The partial pressure of O_2 at 50% saturation (P_{50}) and the slope of the Hill plot at 50% saturation, the Hill coefficient (n_{50}), are reported in Table 2. These empirical parameters are independent of any allosteric model and provide insight to the effects of mutations on O_2 equilibrium binding parameters.

OECs were measured in 0.1 M sodium phosphate buffer at pH 7.0 at 20 °C, which matches conditions of the kinetic

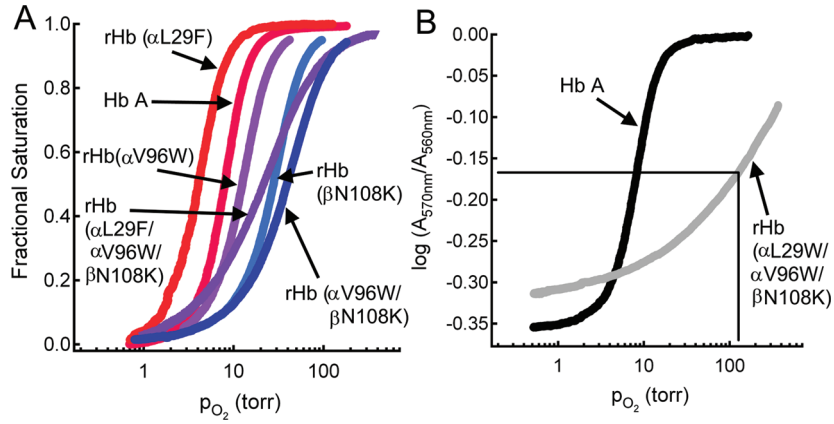

FIGURE 4: Oxygen dissociation curves. P_{50} and the Hill coefficient (n_{50}) values were calculated from curves of (A) Hb A (dark red), rHb (αL29F) (bright red), rHb (αV96W) (light purple), rHb (βN108K) (light blue), rHb (αV96W/βN108K) (dark blue), and rHb (αL29F/αV96W/βN108K) (dark purple). (B) Oxidation of the sample complicated the analysis of rHb (αL29W/αV96W/βN108K), so a raw data set of the O_2 equilibrium binding measurement is presented together with Hb A, with the estimation of P_{50} shown by lines. Experiments were performed in 0.1 M sodium phosphate buffer at pH 7.0 and 20 °C.

experiments, but differs in temperature, pH or both from previously reported binding curves for some of these rHbs. Wiltrout and co-workers reported P_{50} values of 15, 10.9, and 40 Torr for Hb A, rHb (αL29F) and rHb (αL29W) at pH values of 7.0, 6.8 and 7.13, respectively at 29 °C (*35*). Their results match the trend seen in Table 2 and indicate a roughly uniform ~2-fold change in P_{50} due to the 9 °C difference between experimental conditions. Tsai and Ho report P_{50} values of 8.0, 12.8, 24.5 and 48.8 for Hb A, rHb (αV96W), rHb (βN108K) and rHb (αV96W/βN108K), respectively, at pH 7.4 and 29 °C (*51*). This trend of decreasing O_2 affinity is reproduced at pH 7.0 and 20 °C. The effects of pH and temperature on P_{50} appear to compensate each other in these studies, leading to exact matches for the P_{50} values of Hb A and rHb (αV96W) and to close agreement for the rHb (βN108K). The exact compensation between the effects of the pH and temperature is again seen when comparing our results to those of Jeong and co-workers (*29*). Their P_{50} values of 8.0, 4.0, 38 and 22 Torr for Hb A, rHb (αL29F), rHb (αV96W/βN108K) and rHb (αL29F/αV96W/βN108K), respectively, measured at pH 7.4 and 29 °C exactly match our results which were recorded at pH 7.0 and 20 °C.

The equilibrium O_2 binding curve for rHb (αL29W/αV96W/βN108K) is difficult to analyze due to (i) its very low affinity and (ii) its tendency to oxidize during the course of the experiment. Oxidation was estimated by spectral analysis to be <5% for the other Hbs, but was as high as 9% for rHb (αL29W/αV96W/βN108K).

A representative equilibrium oxygen-binding data set for rHb (αL29W/αV96W/βN108K) is shown in Figure 4B along with a binding curve for Hb A collected on the same day. The upper asymptote for the rHb (αL29W/αV96W/βN108K) curve is undefined, and the lower asymptote deviates from that of Hb A. The discrepancy between Hb A and the mutant Hb at low O_2 tensions could be due to oxidation. To account for this oxidation, an asymptotic value for the absorbance of the deoxygenated species was used, which is the average of the deoxy-Hb A lower limit and the lowest mutant deoxy-Hb absorbance value. The upper asymptotic value for the absorbance of fully oxygenated Hb A was used for the mutant protein. These scaling procedures allow estimation of the P_{50} of rHb (αL29W/αV96W/βN108K) as 120 ± 10 Torr in three trials. In addition to altering the absorbance values, oxidation is expected to increase the apparent O_2 affinity of the Hb, suggesting that the O_2 affinity of rHb (αL29W/αV96W/βN108K) may be even lower. Regardless of the exact P_{50} determination, it is clear that these three mutations combine to create a recombinant Hb with dramatically reduced O_2 affinity.

Oxygen affinity is critical in the rational design of a HBOC. The single mutant Hbs affect O_2 affinity either directly, by interfering with ligand binding at the iron atom, or indirectly by altering allostery in the tetramer. The current studies of the combined effects of mutations together with previous reports reveal a relatively simple dependence of P_{50} in the multiple mutant on the P_{50} of each single mutant according to the relationship

$$\text{predicted } P_{50\text{mutations}1+2+3\ldots} = P_{50\text{HbA}} \times \frac{P_{50\text{mutation}1}}{P_{50\text{HbA}}} \times \frac{P_{50\text{mutation}2}}{P_{50\text{HbA}}} \times \frac{P_{50\text{mutation}3}}{P_{50\text{HbA}}} \ldots \quad (2)$$

The effect of each single mutation is expressed as the quotient of the P_{50} value of that single mutant rHb, $P_{50\text{mutation}}$, divided by the P_{50} value of Hb A in the same conditions. The product of these proportionality factors and of the P_{50} of Hb A yields the predicted P_{50} value of a multiply mutated hemoglobin containing each of the single mutations, predicted $P_{50\text{mutations}1+\ 2+3\ldots}$. A plot of the predicted versus measured P_{50} of double- and triple-mutant Hbs is shown in Figure 5. This simple linear relationship is expected to be an oversimplification, and there are relatively few rHbs for which the P_{50} values for both the single and multiple mutants have been measured. However, the correlation is striking and the prediction of the ultralarge P_{50} value of the rHb (αL29W/αV96W/βN108K) triple mutant is remarkably good. These multiple mutants contain substitutions at different regions of the protein, minimizing the potential for direct interference or overlapping effects of mutation. The agreement between the available data points and the line $y = x$ suggests that this relationship may be useful, as a first approximation, for predicting P_{50} values of new multiple mutant Hbs based on the effects of the single mutations. Deviation from the predicted value would indicate a more complicated interaction between the single mutations.

^{1}H NMR Spectra. ^{1}H NMR spectra were collected for samples in the same buffer conditions as were used for

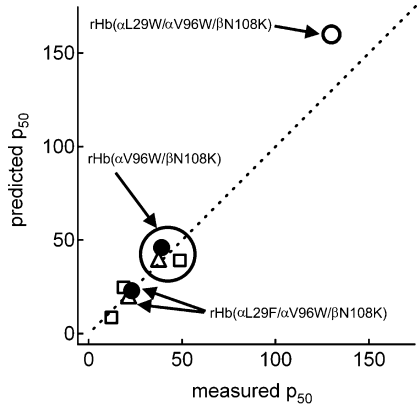

FIGURE 5: Prediction of P_{50} values. Measured P_{50} values for several multiple mutant Hbs are plotted against those predicted by eq 1. The line $y = x$ is provided. Three of the data points refer to separate reports on the same rHb, as indicated. Data cited are from Jeong and co-workers (△) (*29*) and Tsai and Ho (□) (*51*). The rHb (αL29W/αV96W/*β*N108K) point is expected to be an underestimate of the true P_{50} due to oxidation in the sample during the course of the measurement.

kinetic and equilibrium studies, 0.1 M sodium phosphate buffer at pH 7.0 and 20 °C. Figure 6 shows regions of the HbCO spectra featuring exchangeable and ring-current shifted resonances with selected marker peaks labeled. The $\alpha_1\beta_1$ interface was monitored by NεH resonances of α122His and α103His side chains, which arise shifted 12.9 and 12.1 ppm from DSS, respectively (*52*). These two His side chains span the $\alpha_1\beta_1$ interface to contact *β*35Y and *β*131N, respectively, and produce markers conserved in both liganded and deoxy spectra (*19*). The $\alpha_1\beta_2$ interface was monitored by the characteristic R-quaternary state marker at 10.7 ppm. This marker arises from the NεH of the *β*37W side chain and moves from ~10.7 ppm in liganded Hb to ~11.0 ppm in deoxy Hb (*53*). The *β*37W side chain is located within the hinge region of the $\alpha_1\beta_2$ interface, and forms a H-bond with α94D following flash photolysis, early in the R → T transition (*54*). Noble and co-workers systematically replaced over 20 interfacial side chains with Ala and Gly and suggested that the *β*37W−α140Y interaction is the "keystone" of the network stabilizing the T-state conformation (*55*). The distal-heme pocket environment was tracked by the position of the ring-current shifted α62V and *β*67V methyl resonances at −1.8 ppm (*56*). The distal valine side chains approach within 4 Å of the bound O_2 according to a recent X-ray crystal structure determination (pdb accession code 2DN1), and is a sensitive probe of the distal-heme pocket region comprising the O_2 binding site (*57*). A resonance at −1.1 ppm arises from the *β*141L residue (*58*). This side chain is located in the proximal portion of the heme pocket, ~4.5 Å from the proximal histidine, and adjacent to the organic phosphate binding site of the *ββ* cleft. Marker proton resonances of Hb A are labeled in Figure 6.

Spectra of rHb (αL29F) and rHb (αL29W) are unchanged from HbCO A control for markers in the $\alpha_1\beta_1$ and $\alpha_1\beta_2$ interfaces, but show clear shifts in the resonance for α62V, indicating a perturbation to the structure of the α-chain distal-heme pocket environment. These results indicate that the structural consequence of these mutations is local in nature, with the substituted side chains altering the resonance of the nearby distal valine side chain, without extending conformational changes to either $\alpha_1\beta_1$ or $\alpha_1\beta_2$ interface, or the *β*-subunit heme-pocket in the R-state quaternary structure. The large ring-current shift in the mutated α (L29F) subunit suggests, unexpectedly, that the α Phe(B10) side chain causes the Cγ_2 atom of Val62 to move toward the center of the porphyrin ring. Both Hbs containing the αL29F substitution exhibit this upfield shift of for the α62V Cγ_2 resonance. The opposite effect is observed in the Hbs containing αL29W substitutions where the α62V Cγ_2 resonance shows a downfield shift of roughly 0.5 ppm, indicating that the valine side chain is pushed away from the center of the porphyrin ring.

These findings match the trend for aromatic substitutions at helical position B10 reported previously (*29, 35*). Such a direct change to the ligand-binding site is not surprising considering the large sizes of the aromatic side chains and the proximity of the α29L position to both α62V and the bound ligand. The shifts in the resonance of the α62V marker in these single mutants are conserved in rHb (αL29F/αV96W/*β*N108K) and rHb (αL29W/αV96W/*β*N108K).

The αV96W substitution causes three subtle changes in the ^{1}H NMR spectrum of the rHbCO. In the $\alpha_1\beta_2$-interface region, the resonance for the *β*37W side chain is shifted 0.1 ppm downfield, indicating an alteration to the local environment of the *β*37W side chain within the $\alpha_1\beta_2$ interface. This change is accompanied by small shifts of the *β*67V and *β*141L resonances, indicating a change in the heme-pocket of the *β*-chain and showing that this mutation acts across the $\alpha_1\beta_2$ interface to alter the heme-pocket structure of the wild-type partner subunit. A small shift of the α62V marker resonance seems to indicate a perturbation of the α-heme pocket environment, as well. Both markers in the $\alpha_1\beta_1$ interface for rHb (αV96W) are unchanged from those of wild-type Hb A.

We have reported a temperature- and allosteric-effector-dependent appearance of a resonance peak at ~14.2 ppm in the ^{1}H NMR spectrum of rHb (αV96W) (*27*). This peak originates from the H-bond between α42Y and *β*99D in the $\alpha_1\beta_2$ interface of the unliganded T-state molecule, and its emergence reflects a shift in the quaternary structure of the Hb molecule (*59*). The presence of both the 14-ppm T-state marker and the 10.7 ppm R-state marker indicates an intermediate quaternary state. We have further reported that IHP binding causes an increase in the strength of the T-state marker signal and loss of the R-state marker, indicating that rHb (αV96W) has a propensity to adopt the T-state quaternary structure even while fully saturated with CO (*27*). Thus, the structural perturbations noted in Figure 6 indicate a population which is not uniformly in the normal R-state quaternary structure, but is tending toward the T-state structure.

The *β*N108K substitution clearly and dominantly perturbs the $\alpha_1\beta_1$ interface, as seen in the ~0.25 ppm upfield shift of the α103H marker. Figure 6 shows that this feature is conserved in each mutant containing the *β*N108K mutation. Acharya and co-workers found a similar perturbation in $\alpha_1\beta_1$ interface of Tg-Hb Presbyterian, which is Hb containing the *β*N108K substitution, and expressed in a transgenic pig (*21*). Alteration of the α103H marker has been reported for rHb (*β*N108Q), rHb (*β*N108R), and rHb (*β*N108E) indicating a role for the naturally occurring Asn side chain in the structure of the normal R-state $\alpha_1\beta_1$ dimers, and demonstrating the dominant nature of this mutation on the structure of the

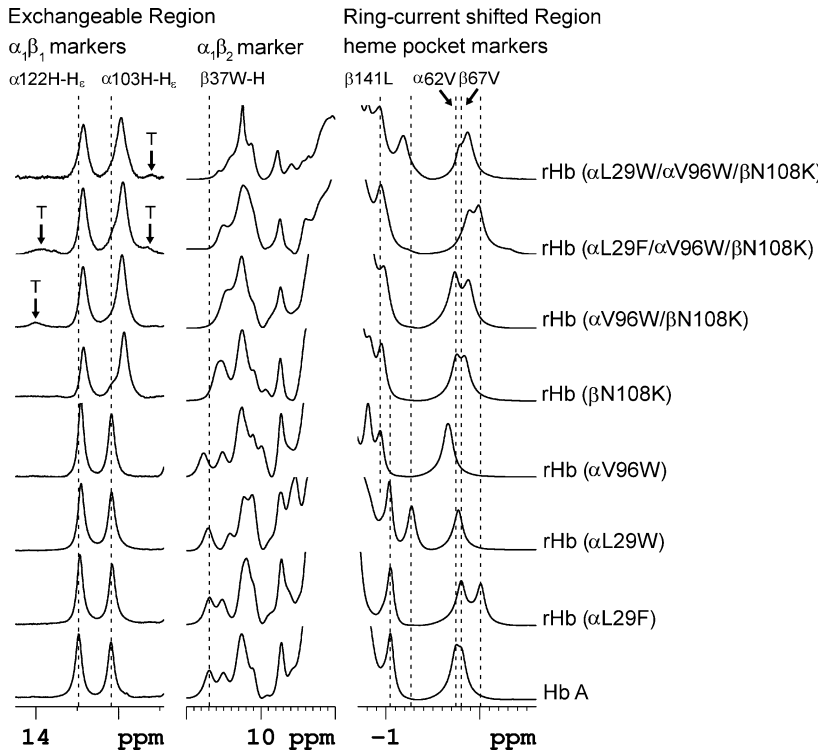

FIGURE 6: ^{1}H NMR spectra of Hbs in 100% CO gas. Hb solutions of 60 mg/mL in 0.1 M phosphate buffer at pH 7.0 were measured at 20 °C. Positions of marker peaks in the heme pocket, $\alpha_1\beta_1$ interface and $\alpha_1\beta_2$ interface are indicated. Positions of marker peaks characteristic of the deoxy structure of hemoglobin are labeled T, and these markers monitor the $\alpha_1\beta_2$ interface.

protein (*51*). In addition to the shift in the α103H resonance, the *β*N108K substitution induces a change in the characteristic R-quaternary state marker at 10.7 ppm, which is associated with *β*37W in the $\alpha_1\beta_2$ interface of HbCO A. In rHb (*β*N108K), this peak appears to have shifted upfield, indicating a marked change in the environment of *β*37W in the $\alpha_1\beta_2$ interface, implying communication between the two major dimer interfaces in the tetrameric Hb A.

Third, there is a small, downfield shift of the *β*141L resonance in the ring-current shifted region for the *β*N108K substitution, indicating a structural perturbation in the vicinity of the proximal side of the heme group. This structural feature exactly matches that seen in the rHb (αV96W) spectrum for the *β*141L marker of the *β*-subunit proximal heme-pocket area. Like the αV96W mutation, the *β*N108K substitution also increases the population of the T-state conformation at low temperatures and in the presence of the allosteric effector IHP, as indicated by the emergence of the resonance at 14.2 ppm (*20, 21*). It appears that the structural changes resulting from the *β*N108K substitution shown in Figure 6 propagate from the site of the mutation in the $\alpha_1\beta_1$ interface to both the $\alpha_1\beta_2$ interface and heme-pocket regions of the liganded molecule, promoting conversion to the T-state structure. Again, this propagation is expected for an "allosteric" mutation.

The rHbs containing both distal-heme pocket and interface mutations reflect the cumulative structural effects of their constituent single mutations. The two $\alpha_1\beta_1$-interface markers of rHb (αV96W/*β*N108K), rHb (αL29F/αV96W/*β*N108K), and rHb (αL29W/αV96W/*β*N108K) contain structural perturbations seen for the rHb (*β*N108K). In addition, small but distinct peaks are apparent at ∼14 ppm in the spectra of rHb (αV96W/*β*N108K) and rHb (αL29F/αV96W/*β*N108K) and at ∼11.2 ppm in the spectra of rHb (αL29F/αV96W/*β*N108K) and rHb (αL29W/αV96W/*β*N108K). An additive effect of the αV96W and *β*N108K substitutions on the strength of the resonance at 14.2 ppm was noted by Tsai and co-workers, and appears to underlie the appearance of that signal in our spectrum (*20*). The peak evident at 11.2 ppm arises from the α94D−*β*37W H-bond and, like the 14-ppm marker, is also in the region of a characteristic T-state quaternary structural marker. Emergence of these resonances indicates the presence of T-state character in the CO saturated tetramer of all three multiple mutants. This conclusion is supported by the waning of the characteristic R-state marker associated with *β*37W in the three multiple mutants, indicating that the ligand-bound forms of these multiple mutant molecules are not in a normal R-state conformation in 0.1 M phosphate buffer at pH 7.0 and 20 °C. The heme-pocket regions of these three proteins also show the additive effects of the single mutations. The 0.1-ppm downfield shift of the *β*141L resonance shared in the spectra of rHb (αV96W) and rHb (*β*N108K) is conserved in all three multiple mutants. The pattern of migration of the α62V resonance in rHbs containing αL29F and αL29W substitutions is also conserved. The distal-heme pocket marker resonance for αV62 Cγ_2 shifts upfield by ∼0.25 ppm in both αL29F containing mutants, and downfield by 0.45 and 0.55 ppm for all of the αL29W containing mutants.

DISCUSSION

In general, the mutations αL29F, αL29W, αV96W, and *β*N108K can be thought of as producing either direct, local structural and functional changes at the ligand-binding site, which alter the intrinsic properties of that subunit, or of producing indirect, global effects in the tetramer that promote changes from the R- to T-like states. The simplest hypothesis

is that the B10 mutations affect only the distal-heme pocket and that the $\alpha_1\beta_1$- and $\alpha_1\beta_2$-interface mutations affect only the equilibrium between the R- and T-quaternary states. The purpose of this work is to examine that hypothesis and verify whether these effects are additive in multiple mutants that could be potential third-generation blood substitute prototypes.

Distal-heme Pocket Substitutions. Placement of Phe or Trp at position B10 of the α-subunit produced dramatic 40- and 330-fold decreases, respectively, in the rate constant for bimolecular O_2 binding to α-subunits after partial photolysis. In contrast, the rate constants for the wild-type β-subunits are, as expected, relatively unperturbed. These decreases in k'_{O_2} are similar to those observed for the same mutations in sperm whale Mb and are unlikely to be due to changes in the population of the R- and T-states given that T-state rate constants for Hb A are only ~5- to 15-fold smaller than those of the R-state. The Phe (B10) substitution also produces a marked decrease in k_{O_2}, but not k_{CO}, indicating a specific electrostatic interaction of bound O_2 with the positive edges of the phenyl-ring multipole. Similar favorable interactions for the Phe (B10) mutation are seen in recombinant Mb (L29F) (*31*). In contrast to Phe (B10), the large size of the indole ring in the Trp (B10) mutant markedly hinders the binding of all ligands due to unfavorable steric interactions, and this effect dominates, causing marked decreases in O_2 affinity for all Trp (B10) mutants, including both Hb subunits and all Mbs that have been investigated. Thus, there is a balance between favorable electrostatic and unfavorable steric effects for aromatic substitutions at the B10 position. The former results in higher O_2 affinity for the αL29F subunit, but the latter results in a much lower O_2 affinity for the αL29W subunit. Thus, O_2 affinity can be manipulated independently of the O_2 association or NO dioxygenation rate constant, both of which decrease due to filling the distal-heme pocket with the large aromatic side chains. The distal-heme pocket structures of rHb (αL29F) and rHb (αL29W) are clearly perturbed, as observed by changes in the αV62 $C\gamma_2$ resonance in the ring-current shifted region (Figure 6). Changes in the extent of the geminate recombination further indicate that these substitutions modify the structure of the active site. Thus, in both rHbs, the intrinsic O_2 affinity of the altered subunit is changed markedly, but there is no effect on the unmodified β-subunit or on the R-state quaternary structure of the tetramer. The ability to produce changes in the intrinsic affinity of different subunits has the potential to lower the cooperativity as measured by the Hill coefficient (n_{50}). Significant subunit heterogeneity is expected to reduce the apparent cooperativity (*60, 61*). NMR studies have detected subunit heterogeneity of Hb A for the first step of O_2 binding in the presence of organic phosphate (*62*). Table 2 shows that reductions in the n_{50} values are observed for rHbs containing αL29F and αL29W substitutions, as would be expected if the α-subunit has much higher and much lower O_2 affinity, respectively, than its partner β-subunit.

Interface Mutations. The βN108K substitution in the $\alpha_1\beta_1$ interface produces a small slow phase for both O_2 and CO rebinding after partial photolysis (~25% of the total amplitude). The rate constant for this slow phase matches reported values for the first step of the ligand binding to the native Hb A tetramers, which are considered to be the T-state rate constants for O_2 and CO binding. This lowered rate constant does not appear to be due to a change in the intrinsic reactivity of the mutated subunit, as was seen for the B10 mutants, but instead appears to be due to a shift toward the T-quaternary state. The relatively large distances, 15 and 21 Å, between the α-carbon of the βN108K amino acid and the β- and α-subunit iron atoms, respectively, seems to preclude a simple direct effect. The agreement between the values of the faster and slower apparent rate constants and those reported for the R- and T-state Hb A suggests that the partially liganded (Hb_4X_3) form of the mutant rHb is composed of populations of the R- and T-type conformational states, which are not seen in the Hb A control.

Results of the ^{1}H NMR measurements and geminate recombination studies show that the βN108K substitution produces spectral changes indicative of a change in the population of the quaternary structures with only small alterations in the heme-pocket compared to the αL29F and αL29W mutations. Thus, as expected, the βN108K $\alpha_1\beta_1$ mutation acts indirectly through global structural changes in the tetramer, to produce less reactive T-like active sites for slower ligand association, more rapid dissociation, and less geminate rebinding. Supporting this interpretation is our NMR evidence that fully liganded rHb (βN108K) and rHb (αV96W) convert to the T-state-like structure in response to lowered temperatures and upon addition of the allosteric effector IHP (*20, 21, 27*).

The αV96W mutation produces changes that are similar to, but less dramatic than, those of the βN108K replacement. Bimolecular association of O_2 with $Hb_4(O_2)_3$ occurs in two phases, with the slower phase accounting for only 10% of the observed absorbance change, but at a rate similar to that expected for the T-state hemoglobin. This mutation shares with rHb (βN108K) (i) the ability to switch quaternary forms without changing ligation state; (ii) perturbation of the proximal heme-pocket marker at −1.2 ppm; and (iii) lowered O_2 affinity. Unlike rHb (βN108K), rHb (αV96W) shows no changes for the $\alpha_1\beta_1$-interface ^{1}H NMR markers. Thus, a perturbed $\alpha_1\beta_1$ interface is not necessary for the ability to switch quaternary forms independent of the ligation state. However, the correlation between the shifts in the −1.2 ppm resonance raises the possibility that perturbation of the β141L marker is linked to alterations at the $\alpha_1\beta_2$ interface.

Effects of Mutations on the Allosteric Transition. As described above, both rHb (βN108K) and rHb (αV96W) can convert to the T-state in fully liganded tetramers at lowered temperatures and upon addition of the allosteric effector IHP (*20, 21, 27*). The ability to switch quaternary conformation, even while fully saturated, is increased when these two mutations are combined in rHb (αV96W/βN108K) (*51*). This propensity is reflected in the ^{1}H NMR spectra in Figure 6, which show increased perturbation compared to the native R-state-like structure according to the trend αV96W/βN108K > βN108K > αV96W >Hb A. Table 2 shows that P_{50} follows the same trend, indicating, as expected, that lowered O_2 affinity coincides with increased ability to access the T-state conformation. This trend is evident in the cooperativity of O_2 binding, measured as the Hill coefficient (n_{50}). The value of n_{50} diminishes as the molecule exhibits greater T-state character in the presence of saturating ligand concentrations. Also, in the partial photolysis ligand rebinding measurements, the increases in amplitude of the slow bimolecular T-state phases and the decreases in the extent of geminate rebinding for O_2 and CO follow the same trend.

The molecular code model developed by Ackers and co-workers describes O_2 binding to Hb in terms of a series of intermediate steps involving intradimer cooperativity and a role for the $\alpha_1\beta_1$ interface in influencing the overall O_2 binding reaction (*14, 15*). Our results for rHb (βN108K) show that the perturbation of the $\alpha_1\beta_1$ interface can affect O_2 binding by acting upon the allosteric transition, supporting the idea of an important role of this interface in the overall reaction. In addition, the ^{1}H NMR spectra of all rHbs containing the βN108K substitution display a shift in the resonance at -1.2 ppm, indicating that the liganded structure of these mutant Hbs differs from the normal R-state structure of Hb A. However, the most important result is that the effects of the $\alpha_1\beta_1$- and $\alpha_1\beta_2$-interface mutants are additive, a result that is important for engineering ligand-binding properties in Hb-based blood substitutes.

Blood Substitute Design. The appropriate O_2 affinity for an Hb-based O_2 carrier (HBOC) remains controversial. Hb A serves as an O_2 delivery agent, with its transport capabilities maximal at its P_{50}, which is ~28 Torr in blood. Normal capillaries have P_{O_2} of ~20 to 30 Torr (*33, 34*), supporting the view that as free O_2 diffuses from the capillary, it is quickly replenished from the store of HbO_2 within RBCs. A high-affinity rHb ($P_{50} < 10$ Torr) will remain saturated at these normal P_{O_2} values. Conversely, a low-affinity rHb, such as rHb (αL29W/αV96W/βN108K), may not fully saturate in the lung and will start to desaturate at higher P_{O_2} values similar to those found in arterioles and large arteries, resulting in premature O_2 delivery. Thus, for Hb in RBCs, a P_{50} of 20 to 30 Torr is optimal and most workers feel that the same logic applies to extracellular HBOCs. However, this view has been challenged (*63*). Extracellular HBOCs have no unstirred layers surrounding them, permeate the cell-free plasma layer lining the vessel walls of arteries and arterioles, and as result, deliver oxygen two to three times more efficiently on an iron basis than RBCs alone (*24*). To prevent premature and excessive O_2 delivery by HBOCs, Cole and co-workers suggest that a $P_{50} < 15$ Torr is optimal for HBOC (*26*). Otherwise the excess O_2 delivery will cause overcompensating autoregulatory responses that will cause vasoconstriction. These workers have argued that the hypertensive side effect of all first generation HBOCs is due to this problem of too much O_2 delivery.

However, Doherty and co-workers examined the hypertensive side-effect of a large number of rHb mutants that had been well characterized with respect to O_2 binding and NO scavenging, including *in-vitro* measurements of the rate constants for NO dioxygenation. They showed a striking correlation between $k'_{NO,ox}$ (from 2 to 70 μM^{-1} s^{-1}) and change in mean arterial pressure (ΔMAP) in 10% top-load, rat model. On the other hand, there was no correlation between P_{50} and ΔMAP for a set of rHbs with P_{50} values ranging from 3 to 50 Torr (*32, 64*). These findings strongly suggest that NO scavenging is the underlying cause of the hypertensive effect.

Our long-term goal is to limit the rate of NO dioxygenation through mutation of the distal-heme pocket with large amino acid side chains, while adjusting P_{50} values to a range of 20 to 30 Torr for optimal O_2 transport in a normal capillary. In previous work, Olson, Doyle, Lemon, and others have shown that replacement of Leu (B10) and Val (E11) with Phe and Trp can markedly reduce the rate of NO dioxygenation (*30, 32, 64*). In this work, we have shown that O_2 affinity is profoundly altered by the Phe (B10) and Trp (B10) mutations in the α-subunits, but through adjustments to $\alpha_1\beta_1$ and $\alpha_1\beta_2$ interfaces that alter the allosteric equilibrium, the P_{50} values of the distal-heme pocket mutants can be readjusted to more favorable values, particularly in the case of the αL29F mutant.

Cooperativity in O_2 binding is decreased in the mutant rHbs in the order Hb A > rHb (αL29F) ≈ rHb (αV96W) ≈ rHb (βN108K > rHb (αL29W) > rHb (αV96W/βN108K) > rHb (αL29F/αV96W/βN108K) > rHb (αL29W/αV96W/βN108K). There are two trends within this overall variation. First, in comparing the distal-pocket mutants rHb (αL29F) and rHb (αL29W), the rHb with the greater subunit difference in the O_2 affinity, rHb (αL29W), also exhibits the largest decrease in the n_{50} value. Second, the rHbs showing the greatest manifestation of the T-state functional and structural traits, even when liganded, also exhibit low n_{50} values because little switching to the high-affinity state occurs until after all four ligands have been bound. In principle, high cooperativity is desired in a HBOC in order to provide more efficient O_2 delivery over small changes in the P_{O_2} values. Our mutants show that the cooperativity is reduced by either markedly increasing or decreasing the affinity of one subunit versus the other causing ordered addition of O_2 with little change in the affinity even with a quaternary transition or by inhibiting the allosteric transition from low- to high-affinity quaternary structure.

In the triple mutant rHb (αL29F/αV96W/βN108K), inhibition of the T to R transition by the two interface mutations compensates for the intrinsic increase in O_2 affinity caused by the αL29F substitution. The resultant triple mutant has a moderate overall affinity, low rates of auto-oxidation, and presumably low rates of NO scavenging by the α-subunit. Thus, it serves as a promising prototype HBOC molecule. In contrast, the triple mutant with the αTrp (B10) replacement, rHb (αL29W/αV96W/βN108K), starts with an intrinsically low affinity of the α-subunits and, when combined with the interface mutations, results in a molecule that is not saturated in air. Perhaps the most remarkable result of this study is that the effects of the single distal-heme pocket and interface mutations are additive and their individual properties can be used to predict those of the multiple mutants. These correlations are highly encouraging for using rational protein engineering and our library of single-point mutations to design safer, more efficient, and more stable HBOCs.

REFERENCES

1. Monod, J., Wyman, J., and Changeux, J. P. (1965) On the nature of allosteric transitions: a plausible model. *J. Mol. Biol. 12*, 88–118.
2. Perutz, M. F., Wilkinson, A. J., Paoli, M., and Dodson, G. G. (1998) The stereochemical mechanism of the cooperative effects in hemoglobin revisited. *Annu. Rev. Biophys. Biomol. Struct. 27*, 1–34.
3. Silva, M. M., Rogers, P. H., and Arnone, A. (1992) A third quaternary structure of human hemoglobin A at 1.7-Å resolution. *J. Biol. Chem. 267*, 17248–17256.
4. Safo, M. K., and Abraham, D. J. (2005) The enigma of the liganded hemoglobin end state: a novel quaternary structure of human carbonmonoxy hemoglobin. *Biochemistry 44*, 8347–8359.

5. Lukin, J. A., Kontaxis, G., Simplaceanu, V., Yuan, Y., Bax, A., and Ho, C. (2003) Quaternary structure of hemoglobin in solution. *Proc. Natl. Acad. Sci. U.S.A. 100*, 517–520.
6. Gong, Q., Simplaceanu, V., Lukin, J. A., Giovannelli, J. L., Ho, N. T., and Ho, C. (2006) Quaternary structure of carbonmonoxyhemoglobins in solution: structural changes induced by the allosteric effector inositol hexaphosphate. *Biochemistry 45*, 5140–5148.
7. Srinivasan, R., and Rose, G. D. (1994) The T-to-R transformation in hemoglobin: a reevaluation. *Proc. Natl. Acad. Sci. U.S.A. 91*, 11113–11117.
8. Bruno, S., Bonaccio, M., Bettati, S., Rivetti, C., Viappiani, C., Abbruzzetti, S., and Mozzarelli, A. (2001) High and low oxygen affinity conformations of T state hemoglobin. *Protein Sci. 10*, 2401–2407.
9. Shibayama, N., and Saigo, S. (2001) Direct observation of two distinct affinity conformations in the T state human deoxyhemoglobin. *FEBS Lett. 492*, 50–53.
10. Samuni, U., Roche, C. J., Dantsker, D., Juszczak, L. J., and Friedman, J. M. (2006) Modulation of reactivity and conformation within the T-quaternary state of human hemoglobin: the combined use of mutagenesis and sol-gel encapsulation. *Biochemistry 45*, 2820–2835.
11. Sahu, S. C., Simplaceanu, V., Gong, Q., Ho, N. T., Tian, F., Prestegard, J. H., and Ho, C. (2007) Insights into the solution structure of human deoxyhemoglobin in the absence and presence of an allosteric effector. *Biochemistry 46*, 9973–9980.
12. Imai, K., Tsuneshige, A., and Yonetani, T. (2002) Description of hemoglobin oxygenation under universal solution conditions by a global allostery model with a single adjustable parameter. *Biophys. Chem. 98*, 79–91.
13. Yonetani, T., Park, S. I., Tsuneshige, A., Imai, K., and Kanaori, K. (2002) Global allostery model of hemoglobin. Modulation of O(2) affinity, cooperativity, and Bohr effect by heterotropic allosteric effectors. *J. Biol. Chem. 277*, 34508–34520.
14. Goldbeck, R. A., Esquerra, R. M., Holt, J. M., Ackers, G. K., and Kliger, D. S. (2004) The molecular code for hemoglobin allostery revealed by linking the thermodynamics and kinetics of quaternary structural change. 1. Microstate linear free energy relations. *Biochemistry 43*, 12048–12064.
15. Goldbeck, R. A., Esquerra, R. M., Kliger, D. S., Holt, J. M., and Ackers, G. K. (2004) The molecular code for hemoglobin allostery revealed by linking the thermodynamics and kinetics of quaternary structural change. 2. Cooperative free energies of (alphaFeCObetaFe)2 and (alphaFebetaFeCO)2 T-state tetramers. *Biochemistry 43*, 12065–12080.
16. Doyle, M. L., and Ackers, G. K. (1992) Cooperative oxygen binding, subunit assembly, and sulfhydryl reaction kinetics of the eight cyanomet intermediate ligation states of human hemoglobin. *Biochemistry 31*, 11182–11195.
17. Henry, E. R., Bettati, S., Hofrichter, J., and Eaton, W. A. (2002) A tertiary two-state allosteric model for hemoglobin. *Biophys. Chem. 98*, 149–164.
18. Olson, J. S., and Maillett, D. H. (2006) Designing a recombinant hemoglobin for use as a blood substitute, in *Blood Substitutes* (Winslow, R., Ed.) pp 354−374, Elsevier, New York.
19. Moo-Penn, W. F., Wolff, J. A., Simon, G., Vacek, M., Jue, D. L., and Johnson, M. H. (1978) Hemoglobin Presbyterian: beta108 (G10) asparagine leads to lysine, A hemoglobin variant with low oxygen affinity. *FEBS Lett. 92*, 53–56.
20. Tsai, C. H., Shen, T. J., Ho, N. T., and Ho, C. (1999) Effects of substitutions of lysine and aspartic acid for asparagine at beta 108 and of tryptophan for valine at alpha 96 on the structural and functional properties of human normal adult hemoglobin: roles of alpha 1 beta 1 and alpha 1 beta 2 subunit interfaces in the cooperative oxygenation process. *Biochemistry 38*, 8751–8761.
21. Acharya, S. A., Malavalli, A., Peterson, E., Sun, P. D., Ho, C., Prabhakaran, M., Arnone, A., Manjula, B. N., and Friedman, J. M. (2003) Probing the conformation of hemoglobin Presbyterian in the R-state. *J. Protein Chem. 22*, 221–230.
22. Looker, D., Abbott-Brown, D., Cozart, P., Durfee, S., Hoffman, S., Mathews, A. J., Miller-Roehrich, J., Shoemaker, S., Trimble, S., Fermi, G., et al. (1992) A human recombinant haemoglobin designed for use as a blood substitute. *Nature 356*, 258–260.
23. Kroeger, K. S., and Kundrot, C. E. (1997) Structures of a hemoglobin-based blood substitute: insights into the function of allosteric proteins. *Structure 5*, 227–237.
24. Page, T. C., Light, W. R., and Hellums, J. D. (1998) Prediction of microcirculatory oxygen transport by erythrocyte/hemoglobin solution mixtures. *Microvasc. Res. 56*, 113–126.
25. Dou, Y., Maillett, D. H., Eich, R. F., and Olson, J. S. (2002) Myoglobin as a model system for designing heme protein based blood substitutes. *Biophys. Chem. 98*, 127–148.
26. Cole, R. H., Vandegriff, K. D., Szeri, A. J., Savaş, O., Baker, D. A., and Winslow, R. M. (2007) A quantitative framework for the design of acellular hemoglobins as blood substitutes: implications of dynamic flow conditions. *Biophys. Chem. 128*, 63–74.
27. Kim, H. W., Shen, T. J., Sun, D. P., Ho, N. T., Madrid, M., and Ho, C. (1995) A novel low oxygen affinity recombinant hemoglobin (alpha96Val→ Trp): switching quaternary structure without changing the ligation state. *J. Mol. Biol. 248*, 867–882.
28. Puius, Y. A., Zou, M., Ho, N. T., Ho, C., and Almo, S. C. (1998) Novel water-mediated hydrogen bonds as the structural basis for the low oxygen affinity of the blood substitute candidate rHb(alpha 96Val→Trp). *Biochemistry 37*, 9258–9265.
29. Jeong, S. T., Ho, N. T., Hendrich, M. P., and Ho, C. (1999) Recombinant hemoglobin(alpha 29leucine → phenylalanine, alpha 96valine → tryptophan, beta 108asparagine → lysine) exhibits low oxygen affinity and high cooperativity combined with resistance to autoxidation. *Biochemistry 38*, 13433–13442.
30. Eich, R. F., Li, T., Lemon, D. D., Doherty, D. H., Curry, S. R., Aitken, J. F., Mathews, A. J., Johnson, K. A., Smith, R. D., Phillips, G. N., Jr., and Olson, J. S. (1996) Mechanism of NO-induced oxidation of myoglobin and hemoglobin. *Biochemistry 35*, 6976–6983.
31. Carver, T. E., Brantley, R. E., Jr., Singleton, E. W., Arduini, R. M., Quillin, M. L., Phillips, G. N., Jr., and Olson, J. S. (1992) A novel site-directed mutant of myoglobin with an unusually high O2 affinity and low autooxidation rate. *J. Biol. Chem. 267*, 14443–14450.
32. Olson, J. S., Foley, E. W., Rogge, C., Tsai, A. L., Doyle, M. P., and Lemon, D. D. (2004) NO scavenging and the hypertensive effect of hemoglobin-based blood substitutes. *Free Radical Biol. Med. 36*, 685–697.
33. Alpert, N. M., Buxton, R. B., Correia, J. A., Katz, P. M., and Ackerman, R. H. (1988) Measurement of end-capillary PO2 with positron emission tomography. *J. Cereb. Blood Flow Metab. 8*, 403–410.
34. Intaglietta, M., Johnson, P. C., and Winslow, R. M. (1996) Microvascular and tissue oxygen distribution. *Cardiovasc. Res. 32*, 632–643.
35. Wiltrout, M. E., Giovannelli, J. L., Simplaceanu, V., Lukin, J. A., Ho, N. T., and Ho, C. (2005) A biophysical investigation of recombinant hemoglobins with aromatic B10 mutations in the distal heme pockets. *Biochemistry 44*, 7207–7217.
36. Shen, T. J., Ho, N. T., Simplaceanu, V., Zou, M., Green, B. N., Tam, M. F., and Ho, C. (1993) Production of unmodified human adult hemoglobin in Escherichia coli. *Proc. Natl. Acad. Sci. U.S.A. 90*, 8108–8112.
37. Shen, T. J., Ho, N. T., Zou, M., Sun, D. P., Cottam, P. F., Simplaceanu, V., Tam, M. F., Bell, D. A., Jr., and Ho, C. (1997) Production of human normal adult and fetal hemoglobins in Escherichia coli. *Protein Eng. 10*, 1085–1097.
38. Olson, J. S., Foley, E. W., Maillett, D. H., and Paster, E. V. (2003) Measurement of rate constants for reactions of O_2, CO, and NO with hemoglobin. *Methods Mol. Med. 82*, 65–91.
39. Mathews, A. J., and Olson, J. S. (1994) Assignment of rate constants for O_2 and CO binding to alpha and beta subunits within R- and T-state human hemoglobin. *Methods Enzymol. 232*, 363–386.
40. Mathews, A. J., Rohlfs, R. J., Olson, J. S., Tame, J., Renaud, J. P., and Nagai, K. (1989) The effects of E7 and E11 mutations on the kinetics of ligand binding to R state human hemoglobin. *J. Biol. Chem. 264*, 16573–16583.
41. Plateau, P., and Gueron, M. (1982) Exchangeable proton NMR without base-line distortion, using new strong-pulse sequences. *J. Am. Chem. Soc. 104*, 7310–7311.

42. Maillett, D. H. Engineering hemoglobins and myoglobins for efficient O_2 transportPh.D. diss., Rice University, Houston, TX, 2003.
43. Springer, B. A., Sligar, S. G., Olson, J. S., and Phillips, G. N. (1994) Mechanisms of Ligand Recognition in Myoglobin. *Chem. Rev. 94*, 699–714.
44. Unzai, S., Eich, R., Shibayama, N., Olson, J. S., and Morimoto, H. (1998) Rate constants for O_2 and CO binding to the alpha and beta subunits within the R and T states of human hemoglobin. *J. Biol. Chem. 273*, 23150–23159.
45. Shibayama, N., Yonetani, T., Regan, R. M., and Gibson, Q. H. (1995) Mechanism of ligand binding to Ni(II)-Fe(II) hybrid hemoglobins. *Biochemistry 34*, 14658–14667.
46. Gibson, Q. H. (1999) Kinetics of oxygen binding to hemoglobin A. *Biochemistry 38*, 5191–5199.
47. Murray, L. P., Hofrichter, J., Henry, E. R., Ikeda-Saito, M., Kitagishi, K., Yonetani, T., and Eaton, W. A. (1988) The effect of quaternary structure on the kinetics of conformational changes and nanosecond geminate rebinding of carbon monoxide to hemoglobin. *Proc. Natl. Acad. Sci. U.S.A. 85*, 2151–2155.
48. Hirota, S., Li, T. S., Phillips, G. N. J., Olson, J. S., and Kitagawa, T. (1996) Perturbation of the Fe-O_2 bond by nearby residues in heme pocket - observation of nu(Fe-O_2) Raman bands for oxymyoglobin mutants. *J. Am. Chem. Soc. 118*, 7845–7846.
49. Olson, J. S. (1981) Stopped-flow, rapid mixing measurements of ligand binding to hemoglobin and red cells. *Methods Enzymol. 76*, 631–651.
50. Olson, J. S., Rohlfs, R. J., and Gibson, Q. H. (1987) Ligand recombination to the alpha and beta subunits of human hemoglobin. *J. Biol. Chem. 262*, 12930–12938.
51. Tsai, C. H., and Ho, C. (2002) Recombinant hemoglobins with low oxygen affinity and high cooperativity. *Biophys. Chem. 98*, 15–25.
52. Simplaceanu, V., Lukin, J. A., Fang, T. Y., Zou, M., Ho, N. T., and Ho, C. (2000) Chain-selective isotopic labeling for NMR studies of large multimeric proteins: application to hemoglobin. *Biophys. J. 79*, 1146–1154.
53. Fang, T. Y., Simplaceanu, V., Tsai, C. H., Ho, N. T., and Ho, C. (2000) An additional H-bond in the alpha 1 beta 2 interface as the structural basis for the low oxygen affinity and high cooperativity of a novel recombinant hemoglobin (beta L105W). *Biochemistry 39*, 13708–13718.
54. Goldbeck, R. A., Esquerra, R. M., and Kliger, D. S. (2002) Hydrogen bonding to Trp beta37 is the first step in a compound pathway for hemoglobin allostery. *J. Am. Chem. Soc. 124*, 7646–7647.
55. Noble, R. W., Hui, H. L., Kwiatkowski, L. D., Paily, P., DeYoung, A., Wierzba, A., Colby, J. E., Bruno, S., and Mozzarelli, A. (2001) Mutational effects at the subunit interfaces of human hemoglobin: evidence for a unique sensitivity of the T quaternary state to changes in the hinge region of the alpha 1 beta 2 interface. *Biochemistry 40*, 12357–12368.
56. Dalvit, C., and Ho, C. (1985) Proton nuclear Overhauser effect investigation of the heme pockets in ligated hemoglobin: conformational differences between oxy and carbonmonoxy forms. *Biochemistry 24*, 3398–3407.
57. Park, S. Y., Yokoyama, T., Shibayama, N., Shiro, Y., and Tame, J. R. (2006) 1.25 Å resolution crystal structures of human haemoglobin in the oxy, deoxy and carbonmonoxy forms. *J. Mol. Biol. 360*, 690–701.
58. Zheng, Y., Giovannelli, J. L., Ho, N. T., Ho, C., and Yang, D. (2004) Side-chain assignments of methyl-containing residues in a uniformly 13C-labeled hemoglobin in the carbonmonoxy form. *J. Biomol. NMR 30*, 423–429.
59. Fung, L. W., and Ho, C. (1975) A proton nuclear magnetic resonance study of the quaternary structure of human homoglobins in water. *Biochemistry 14*, 2526–2535.
60. Dahlquist, F. W. (1978) The meaning of Scatchard and Hill plots. *Methods Enzymol. 48*, 270–299.
61. Barrick, D., Ho, N., Simplaceanu, V., Dahlquist, F. W., and Ho, C. (1997) A test of the role of the proximal histidines in the Perutz model for cooperativity in haemoglobin. *Nat. Struct. Biol. 4*, 78–83.
62. Viggiano, G., Ho, N. T., and Ho, C. (1979) Proton nuclear magnetic resonance and biochemical studies of oxygenation of human adult hemoglobin in deuterium oxide. *Biochemistry 18*, 5238–5247.
63. Intaglietta, M., Cabrales, P., and Tsai, A. G. (2006) Microvascular perspective of oxygen-carrying and -noncarrying blood substitutes. *Annu. Rev. Biomed. Eng. 8*, 289–321.
64. Doherty, D. H., Doyle, M. P., Curry, S. R., Vali, R. J., Fattor, T. J., Olson, J. S., and Lemon, D. D. (1998) Rate of reaction with nitric oxide determines the hypertensive effect of cell-free hemoglobin. *Nat. Biotechnol. 16*, 672–676.

BI800816V